Published in final edited form as:
Ann Thorac Surg. 2011 August ; 92(2): 617–624. doi:10.1016/j.athoracsur.2011.04.051.

Modification of Infarct Material Properties Limits Adverse Ventricular Remodeling

Masato Morita, MD[2], **Chad E. Eckert, PhD**[4], **Kanji Matsuzaki, MD, PhD**[2], **Mio Noma, MD**[2], **Liam P. Ryan, MD**[1,2], **Jason A. Burdick, PhD**[3], **Benjamin M. Jackson, MD**[1], **Joseph H. Gorman III, MD**[1,2], **Michael S. Sacks, PhD**[4], and **Robert C. Gorman, MD**[1,2]

[1]Department of Surgery, University of Pennsylvania, Philadelphia, PA

[2]Gorman Cardiovascular Research Group, University of Pennsylvania, Philadelphia, PA

[3]Department of Bioengineering, University of Pennsylvania, Philadelphia, PA

[4]Engineered Tissue Mechanics and Mechanobiology Laboratory, Department of Bioengineering, Swanson School of Engineering, McGowan Institute, School of Medicine, University of Pittsburgh, Pittsburgh, PA

Abstract

Background—Studies of the biomechanical response of the left ventricle (LV) to myocardial infarction (MI) have identified infarct expansion as an important phenomenon that both initiates and sustains adverse LV remodeling. We tested the hypothesis that infarct modification via material-induced infarct stiffening and thickening limits infarct expansion and LV remodeling.

Methods—Twenty-one sheep had anteroapical infarction and were randomized to either injection of 2.6ml of saline or 2.6ml of a tissue filler material into the infarct within 3 hours of coronary occlusion. Animals were followed for 8 weeks with echocardiography to assess infarct expansion and global LV remodeling. Post-mortem morphometric measurements were performed on the excised heart to quantify infarct thickness; regional blood flow was assessed with colored microspheres. Infarct material properties were directly measured using biaxial tensile testing.

Results—Treatment animals had less infarct expansion and reduced LV dilatation 8 weeks after MI (LV systolic volumes 60.8±4.3ml vs. 80.3±6.9ml, $p<0.05$). Ejection fraction was greater in the treatment animals (31.0±2.6% vs. 27.6±1.3%, $p<0.05$). The treatment group had thicker infarcts (5.5±0.2mm vs. 2.2±0.3mm, $p<0.05$) and greater infarct blood flow than control groups (0.22±0.04ml/min/g vs. 0.11±0.03ml/min/g, $p<0.05$). The longitudinal peak strain in the treatment group was less (0.05014±0.0141) than the control group (0.1024±0.0101), indicating increased stiffness of the treated infarcts.

Conclusion—Durable infarct thickening and stiffening can be achieved by infarct biomaterial injection resulting in the amelioration of both infarct expansion and global LV remodeling. Further material optimization will allow for clinical translation of this novel treatment paradigm.

Address Correspondence to: Corresponding author: Robert C. Gorman, MD Gorman Cardiovascular Research Group Glenolden Research Laboratory University of Pennsylvania 500 S. Ridgeway Avenue Glenolden, PA 19036 Phone: 267-350-9614 FAX: 267-350-9627 gormanr@uphs.upenn.edu.

Keywords

Biomaterials; Echocardiography; Myocardial Infarction; Myocardial Mechanics; Myocardial Remodeling

Introduction

Studies of the biomechanical response of the left ventricle (LV) to myocardial infarction (MI) have identified infarct expansion (i.e. stretching) as an important phenomenon that both initiates and sustains a progressive pathologic process that ultimately results in LV dilatation, loss of global contractile function, symptomatic heart failure and death.[1–3] This maladaptive infarction-induced ventricular remodeling is a complex process that is, in its initial phase, a largely mechanical problem manifest by abnormal myocardial stress patterns; however, with time these abnormal stress distributions lead to inherent biologic changes in the myocardium that become difficult to reverse by any means once established.[3–6]

Based on the understanding that the mechanical phenomenon of infarct expansion initiates the adverse LV remodeling that leads to heart failure, we hypothesized, over a decade ago, that physical restraint of the infarct would limit adverse remodeling. In a series of experiments using surgical mesh materials in large animal infarct models we confirmed the beneficial effects of mechanically restraining infarcts early after an MI.[7–13] As a result, our group and others have begun to develop and test materials that can be introduced directly into the infarct to prevent its expansion. While several substances have shown promise little work has been performed to optimize material design or to elucidate the mechanism by which infarct expansion is reduced.[14–18]

In this study we tested the hypothesis that infarct modification via material-induced infarct stiffening and thickening limits infarct expansion and LV remodeling. We used a biocompatible, calcium hydroxyapatite-based soft tissue filler to modify the infarct in an ovine anteroapical infarction model.[14]

Materials and Methods

Animal Model

A myocardial infarction was surgically induced in 21 adult male sheep (35–40 kg) using a well-described method.[19] Briefly, the animals were anesthetized and underwent left thoracotomy. An anteroapical infarction was produced by ligating the left anterior descending artery and its diagonal branches, resulting in an infarction of approximately 20% of the LV mass. This technique has been shown to reproducibly create infarctions of a very consistent size. Subsequently, the sheep were randomized in a 1:2 fashion to receive 2.6 ml of either saline or tissue filler within 3 hours of infarction. The injectate was delivered in 20 equally sized boluses spaced evenly over the accessible region of the infarct on the anteroapical region of the LV (Figure 1). The septal component of the infarct was not treated. Six additional animals that did not have an infarction were used in the study to act as referent controls for the dobutamine stress echocardiographic testing, regional blood flow assessments and post-mortem morphometric measurements. All animals were treated and cared for in accordance with the National Institutes of Health “Guide for the Care and Use of Laboratory Animals” (National Research Council, Washington, DC, 1996).

Biocompatible Tissue Filler

Radiesse® (Bioform Medical Inc., San Mateo, CA) is a viscous (gel-like consistency) biocompatible dermal and soft tissue filler of calcium hydroxyapatite microspheres suspended in an aqueous gel carrier of water, glycerin and carboxymethylcellulose. Once injected, fibroblasts grow on and around the microspheres, replacing the carrier over time.[20,21] Radiesse® has been studied in diverse applications including radiopaque tumor marking, bladder neck augmentation, vocal cord injection and cosmetic facial-volume augmentation.[22,23] The material is supplied in 1.3 ml syringes; two syringes were used for each treatment animal.

Echocardiographic Protocol

Transapical epicardial three-dimensional echocardiography was performed through a left thoracotomy immediately prior to MI, 30 minutes after MI and 15 minutes after injection in all subjects. Transdiaphragmatic echocardiography was performed at 8 weeks after MI at resting conditions and after 5mcg/kg/min of dobutamine was administered. All echocardiograms were recorded using a Philips iE 33 platform with a 7 MHz ultrasound probe (Philips, Bothell, WA). Full volume 3D data were acquired. These datasets were exported for offline analysis using QLAB software (Philips, Bothell, WA). The three-dimensional image acquired was manipulated to display two orthogonally related long axis views, bisecting each other on the central long axis of the left ventricle. End diastole (ED) was defined as the frame prior to closure of the mitral valve and end systole (ES) as the frame prior to closure of the aortic valve. For each of these two time points, end diastolic left ventricular volume (EDV), end systolic left ventricular volume (ESV) and ejection fraction (EF) were obtained according to the software manufacturer's recommended method. Myocardial infarct length (wall motion abnormality length in long axis) was also measured. All image analysis was performed by a blinded analyst.

Hemodynamic Measurements

A pulmonary artery catheter was placed to allow for the measurement of cardiac output (CO) by means of thermodilution as well as central venous pressure (CVP). A high fidelity pressure transducer was also placed in the LV to assess LV end diastolic pressure. Hemodynamic data were recorded immediately prior to the echocardiographic studies.

Regional Blood Flow Measurements

In all infarcted animals as well as in 6 normal uninfarcted animals, fifteen million color-coded, 15.5 μm diameter NuFlow Fluorescent microspheres (IMT Laboratories, Irvine, CA) were injected during the terminal study under resting conditions and after dobutamine was administered. Reference blood samples were taken at both time points. Reference blood samples and myocardial specimens from the infarct, adjacent borderzone and remote regions were analyzed using flow cytometry for microsphere content by IMT Laboratories. Regional perfusion was calculated using the following formula: $Q_m = (C_m \times Q_r)/Cr$, where Q_m = myocardial blood flow per gram (ml/min/g) of sample, C_m = microsphere count per gram of tissue in sample, Q_r = withdrawal rate of the reference blood sample (ml/min) and C_r = microsphere count in the reference blood sample.

Post-Mortem Morphometric Assessment

Animals were sacrificed after the final microsphere injection. The heart was then excised and the LV was opened through the septum and a standardized digital photo was taken (Casio EX-Z850, Tokyo Japan). All photographs were imported into an image analysis program (Image Pro Plus, Media Cybernetics; Silver Spring, MD) and computerized planimetry was performed to assess the size of the infarct.[15] The infarct area was

expressed as a percentage of the left ventricle area. The right ventricle and left ventricle were weighed individually. A 15mm square section of infarct tissue taken from the center of the infarct was excised for biaxial mechanical testing. The myocardial thickness was measured in the most apical portion of the infarct, the most basilar portion of the infarct, the borderzone and remote region with a digital micrometer. The infarct tissue was fixed and stained with Masson's trichrome.

Mechanical Testing of Infarct Tissue

All mechanical testing was performed using a biaxial tensile mechanical testing device.[24] Custom software permitted the precise control of applied load to both axes and tracked fiducial markers. Specimens were preconditioned to a 10 kPa peak equibiaxial stress for fifteen cycles with a fifteen second half cycle time. A one gram tare was used as the testing reference state, though post-preconditioned free-floating reference states were obtained for post-processing analyses. Equibiaxial mechanical testing to a 10 kPa peak stress was performed on all specimens for ten cycles at a fifteen second half cycle time.

A finite-element based surface interpolation technique was employed to determine the two-dimensional in-surface Eulerian strain tensor “e” at each time point.[25] A single four-node linear Lagrangian element was employed. In order to reference the deformed state configuration and calculate “e”, a convective, in-surface coordinate system was used in which the axes were aligned to the local longitudinal and circumferential directions of the myocardium. In this analysis, the Eulerian strain tensor components were computed at each load iteration. Additionally, the second Piola-Kirchhoff stress was computed using the deformation gradient tensor. Strain energy was computed using the trapezoidal rule for both circumferential and radial directions.

Statistical Analysis

Measurements are reported as means ± standard errors of the mean. For the echocardiographic and hemodynamic data between-group differences are compared by analysis of variance for repeated measures. If analysis of variance (ANOVA) revealed significant differences, Student's t-test with the Bonferroni correction was used to assess differences between groups at specific time points post infarction (SPSS, Chicago, Illinois).

For mechanical testing of the infarct tissue raw data was compiled, consisting of peak directional strains and direction and total strain energies, for each group. Statistically significant differences were assessed using a one-way ANOVA test. In all cases significance was assumed at $p < 0.05$.

Results

Animal Survival

One animal in the control group and two animals in the treatment group died of intractable ventricular arrhythmias within an hour of coronary occlusion before injection of the tissue filler or saline. One treatment animal died approximately 24 hours after infarction of a presumed arrhythmia. Six control animals and 11 treatment animals completed the study without further complications.

Left Ventricular Remodeling

Echocardiographic data are presented in Table 1. None of the baseline echocardiographic parameters were statistically different between the groups. Immediately after infarction both groups experienced LV dilatation. ESV and EDV were similar in both groups and increased significantly relative to pre-infarction. The initial length of the apical wall motion

abnormality was 7.2±0.3cm in the control group and 7.1±0.3cm in the treatment group confirming that the initial infarct size was comparable in both groups. Both groups experienced significant LV dilatation during the 8 week study period; however, both ESV (60.8±4.3ml vs. 80.3±6.9ml) and EDV (87.2±4.0ml vs. 110.6±8.4ml) where significantly smaller in the treatment group. While EF also decreased significantly in both groups, it was significantly higher in the treatment group at 8 weeks after infarction (31.0±2.6% vs. 27.6±1.3%). ESV and EDV decreased significantly and EF increased significantly in both groups after the administration of dobutamine; however, the differences between groups persisted. Infarct length was significantly smaller in the treatment group at 8 weeks after MI, consistent with reduced infarct expansion (8.0±0.2cm vs. 9.3±0.6cm).

In addition to experiencing less LV dilatation the treatments animals also demonstrated a trend toward preservation of the normal elliptical shape of the ovine heart. (Figure 2)

Hemodynamic Data

Hemodynamic data are presented in Table 1. Cardiac output was higher in the treatment group at 8 weeks after infarction both before (4.2±0.2l/m vs. 2.7±0.1l/m) and after the administration of dobutamine (6.0±0.3l/m vs. 4.8±0.9l/m). LV diastolic pressures were not significantly different in the control (12.3±1.1mmHg) and treatment (9.8±2.4mmHg) groups 8 weeks after infarction.

Regional Myocardial Blood Flow

Regional myocardial blood flow data are presented in Table 2. Blood flow in the infarct region was significantly reduced in the infarct zone relative to the borderzone and remote zone at 8 weeks after infarction in both groups; however, infarct blood flow was significantly higher in the treatment group (0.22±0.04ml/min/g vs. 0.11±0.03ml/min/g). This difference became more pronounced under pharmacologic stress with dobutamine (0.43±0.11ml/min/g vs. 0.14±0.03ml/min/g). Borderzone and remote blood flow in the unstressed state was significantly higher in the control group (0.78±0.11ml/min/g and 0.75±0.14ml/min/g) than in either the treatment group (0.51±0.05ml/min/g and 0.48±0.04ml/min/g) or the normal uninfarcted animals (0.52±0.07ml/min/g and 0.47±0.04ml/min/g). In response to dobutamine-induced stress neither the control group nor the therapy group could increase regional blood flow in uninfarcted myocardial segments to levels achieved in normal animals.

Morphometric and Pathologic Data

Post-mortem cardiac morphometric data are presented in Table 3. When compared to controls treatment group animals had thicker infarcts in the apical aspect of the infarct (2.2±0.3mm vs. 5.5±0.2mm) and in the basilar aspect of the infarct (4.7±0.4mm vs. 7.1±0.2mm, Figure 3). The infarct area in the treatment group was significantly smaller than the control group (25.8±1.3% vs. 28.7±1.0%) which is consistent with a treatment-induced reduction in infarct expansion. Both the treatment group and the control group demonstrated significantly increased LV weights relative to normal animals (137.5±4.3g and 131.8±3.4g vs. 115.0±5.4g), consistent with LV hypertrophy. RV weights were also increased in both groups relative to normal animals.

Masson's trichrome staining demonstrated exuberant collagen production in all treatment group animals relative to control (Figure 4). The increase in collagen correlated well with most of the increased infarct thickness. Eight weeks after infarction the carrier gel had been completely absorbed and a cellular infiltrate was left surrounding the calcium hydroxyapatite microspheres.

Infarct Mechanical Properties

Figure 5 summarize the results of the mechanical testing of the infarct tissue. Longitudinal peak strain was significantly reduced in the treatment group (0.05014±0.0141) compared to the control group (0.1024±0.0101). While a slight decrease in circumferential peak strain was seen in the treatment group the difference did not reach statistical significance. These differential responses resulted in nearly isotropic infarct material properties in the control group in contrast to highly anisotropic condition in the treatment group. Longitudinal peak strain energy was significantly reduced in the treatment group (0.0271±0.0328 kPa) compared to the control group (0.1861 ±0.0289kPa). A statistical difference was not present in circumferential peak strain energy. Total strain energy was also significantly less in the treatment group (0.2757±0.0494 kPa) compared to control (0.4531±0.0519kPa). As with the mean peak strain data, the directional strain energies shifted from isotropic to anisotropic conditions between the treatment and control groups.

Comment

This study demonstrates that injection of a reactive tissue filler agent into the infarct zone within hours of coronary occlusion produces stiffer and thicker infarcts 8 weeks after a large transmural myocardial infarction. This tissue filler material is designed to provoke a tissue response that results in the stimulation of collagen production, resulting in a thickening and stiffening of the myocardial wall. The observed changes in infarct properties were associated reduced infarct expansion, an attenuation of LV remodeling, and improved global LV function. This work builds on our previous study in which we demonstrated that the same tissue filler material limited infarct dyskinetic movement immediately after injection.[14] One unique aspect of the current study is that we employed a state-of-the-art tensile mechanical testing device to directly compare infarct material properties in treated and untreated infarct tissue. Importantly, our data confirm the hypotheses proposed in previously published theoretical and experimental studies that have suggested that stiffening of the infarct region should have beneficial effects on LV remodeling and function.[26, 27, 28] Specifically, infarct thickening and stiffening should result in reduced mechanical stresses not only in the infarct region, but also in the perfused myocardial segments outside the infarct. This has important implications since increased myocardial stress has been identified as stimulus for inherent biologic changes in remodeled myocardium.[29–31]

This study adds to a growing body of literature that support the efficacy of using injectable materials to limit infarct expansion in the early post-MI period.[14–18,32] The significance of pursuing this therapeutic concept is potentially profound, because it raises the distinct possibility of a percutaneous catheter-based direct treatment of the infarct to modify its material properties in the early post-MI period with the intent of limiting or preventing long-term adverse LV remodeling and loss of global contractile function.

As the potential for such a therapeutic paradigm has become apparent, so have the limitations of our current knowledge. A range of injectable biomaterials have been studied, including biological materials such as alginate,[16] fibrin,[33] and derivatives of the ECM, [34] as well as synthetic materials like self-assembling peptides [18] and thermoresponsive n-isopropyl acrylamide (NIPAAM) gels.[35] These materials, as used and delivered with various injection techniques and activation processes (e.g., alginate gels are activated in the presence of divalent cations, whereas NIPAAM gels transition based on temperature), present a very wide range of mechanical, resorptive and tissue reaction properties. In addition most materials tested to date have used common formulations developed for other applications and in many of these materials, there is little control over their physical properties. Thus, there is a need for a material system that can be engineered to optimize stiffness, durability and ease of delivery.

Although the tissue filler used in this experiment demonstrated efficacy in limiting adverse LV remodeling, it is likely suboptimal for clinical use. While remodeling was attenuated it was not prevented; LV dilatation progressed over the eight week follow-up period. Theoretically, an optimally engineered material would prevent progressive infarct expansion and LV dilatation beyond the point where the ventricle has compensated for the loss of contractile myocardium and normalized stroke volume. The high viscosity of this particulate containing filler would also make catheter delivery difficult.

While the infarcts in the treatment group were clearly stiffer than in the control group, the mechanism by which stiffening occurred as well as its time course was likely complex. These are important issues that were not directly addressed in the current study. Immediately after injection the bulk material properties of the injectate likely imparted an increased to stiffness to the infarct region. Over time there was the expected tissue response to the filler in which macrophages cleared the carrier gel and responded to the microspheres to induce an exuberant production of collagen that contributed to the anisotropic infarct stiffening documented by the biaxial mechanical testing.

The material used in this experiment has no known inherent angiogenic properties; therefore, it is likely that the increased blood flow observed in the infarcts of the treated animals was the result of a reactive inflammatory response to the material. This is an important finding because the injection of various cells, genes and gene products into infarcts has been touted as a technique to increase infarct blood flow based on the *in vitro* determinations of the material's angiogenic potential.[36, 37] This study documents that nonspecific responses to injected materials can produce increased infarct blood flow.

In summary, durable infarct thickening and stiffening can be achieved by biomaterial injection into the infarct resulting in the anticipated amelioration in both infarct expansion and global LV remodeling. While much work remains to be accomplished, the requisite catheter technology, imaging modalities and material science expertise exist to make this novel preventative approach to infarction-induced heart failure a clinical reality in the not-too-distant future.

Acknowledgments

This research project was supported by grants from the National Heart, Lung and Blood Institute of the National Institutes of Health, Bethesda, MD, (HL63954 and HL73021). R. Gorman and J. Gorman are supported by individual Established Investigator Awards from the American Heart Association, Dallas, TX.

References

1. Erlebacher JA, Weiss JL, Weisfeldt ML, Bulkley BH. Early dilation of the infarcted segment in acute transmural myocardial-infarction-role of infarct expansion in acute left-ventricular enlargement. Journal of the American College Cardiology. 1984; 4:201–208.
2. Weisman HF, Healy B. Myocardial infarct expansion, infarct extension, and reinfarction - pathophysiologic concepts. Progress in Cardiovascular Diseases. 1987; 30:73–110. [PubMed: 2888158]
3. Jackson BM, Gorman JH, Moainie SL, et al. Extension of borderzone myocardium in postinfarction dilated cardiomyopathy. Journal of the American College of Cardiology. 2002; 40:1160–1167. discussion 1168–1171. [PubMed: 12354444]
4. Kramer CM, Lima JAC, Reichek N, et al. Regional differences in function within noninfarcted myocardium during left-ventricular remodeling. Circulation. 1993; 88:1279–1288. [PubMed: 8353890]

5. Guccione JM, Moonly SM, Moustakidis P, et al. Mechanism underlying mechanical dysfunction in the border zone of left ventricular aneurysm: a finite element model study. Annals of Thoracic Surgery. 2001; 71:654–662. [PubMed: 11235723]
6. Gorman RC, Gorman JH III. Mechanism Underlying Mechanical Dysfunction in the Borderzone Left Ventricular Aneurysm. A Finite Element Model Study. Invited commentary. Annals of Thoracic Surgery. 2001; 71:662.
7. Kelley ST, Malekan R, Gorman JH, et al. Restraining infarct expansion preserves left ventricular geometry and function after acute anteroapical infarction. Circulation. 1999; 99:135–142. [PubMed: 9884390]
8. Moainie SL, Guy TS, Gorman JH III, et al. Infarct Restraint Attenuates Remodeling and Reduces Chronic Ischemic Mitral Regurgitation after Posterolateral Infarction. Annals of Thoracic Surgery. 2002; 74:444–449. discussion 449. [PubMed: 12173827]
9. Pilla JJ, Blom AS, Brockman DJ, et al. Ventricular Constraint Using the Acorn Cardiac Support Device Reduces Myocardial Akinetic Area in an Ovine Model of Acute Infarction. Circulation. 2002; 106(12 Suppl):I207–211. [PubMed: 12354735]
10. Enomoto Y, Gorman JH III, Moainie SL, et al. Early Ventricular Restraint after Myocardial Infarction: Extent of the Wrap Determines the Outcome of Remodeling. Annals of Thoracic Surgery. 2005; 79:881–887. [PubMed: 15734399]
11. Blom AS, Mukherjee R, Pilla JJ, et al. A Cardiac Support Device Modifies Left Ventricular Geometry and Myocardial Structure After Myocardial Infarction. Circulation. 2005; 112:1274–1283. [PubMed: 16129812]
12. Pilla JJ, Blom AS, Gorman JH III, et al. Early Post Infarction Ventricular Restraint Improves Borderzone Wall Thickening Dynamics during Remodeling. Annals of Thoracic Surgery. 2005; 80:2257–2262. [PubMed: 16305885]
13. Blom AS, Pilla JJ, Arkles J, et al. Ventricular restraint prevents infarct expansion and improves borderzone function after myocardial infarction: a study using magnetic resonance imaging, three-dimensional surface modeling, and myocardial tagging. Annals of Thoracic Surgery. 2007; 84:2004–2010. [PubMed: 18036925]
14. Ryan LP, Matsuzaki K, Noma M, et al. Dermal filler injection: a novel approach for limiting infarct expansion. Annals of Thoracic Surgery. 2009; 87:148–155. [PubMed: 19101288]
15. Ifkovits JL, Tous E, Minakawa M, et al. Injectable hydrogel properties influence infarct expansion and extent of postinfarction left ventricular remodeling in an ovine model. Proceedings of the National Academy of Sciences of the United States of America. 2010; 107:11507–11512. [PubMed: 20534527]
16. Leor J, Tuvia S, Guetta V, et al. Intracoronary injection of in situ forming alginate hydrogel reverses left ventricular remodeling after myocardial infarction in swine. Journal of the American College of Cardiology. 2009; 54:1014–1023. [PubMed: 19729119]
17. Yu J, Christman KL, Chin E, et al. Restoration of left ventricular geometry and improvement of left ventricular function in a rodent model of chronic ischemic cardiomyopathy. Journal of Thoracic and Cardiovascular Surgery. 2009; 137(1):180–187. [PubMed: 19154923]
18. Hsieh PC, Davis ME, Gannon J, MacGillivray C, Lee RT. Controlled delivery of pdgf-bb for myocardial protection using injectable self-assembling peptide nanofibers. Journal of Clinical Investigation. 2006; 116:237–248. [PubMed: 16357943]
19. Markovitz LJ, Savage EB, Ratcliffe MB, et al. A large animal model of left ventricular aneurysm. Annals of Thoracic Surgery. 1989; 48:838–845. [PubMed: 2596920]
20. Shimizu SI. Subcutaneous tissue response in rats to injection of fine particles of synthetic hydroxyapatite ceramic. Biomedical Research. 1988; 9:95–111.
21. Drobeck HP, Rothstein SS, Gumaer KI, Sherer AD, Slighter RD. Histologic observation of soft tissue responses to implanted, multifaceted particles and discs of hydroxyapatite. J Oral Maxillofacial Surgery. 1984; 42:143–149.
22. Tzikas TL. Evaluation of the Radiance FN soft tissue filler for facial soft tissue augmentation. Archives Facial and Plastic Surgery. 2004; 6:234–239.

23. Kanchwala SK, Holloway L, Bucky LP. Reliable soft tissue augmentation: a clinical comparison of injectable soft-tissue fillers for facial-volume augmentation. Annals of Plastic Surgery. 2005; 55:30–35. [PubMed: 15985788]
24. Billiar KL, Sacks MS. Biaxial mechanical properties of the natural and glutaraldehyde treated aortic valve cusp--Part I: Experimental results. Journal of Biomechanical Engineering. 122:23–30. 200. [PubMed: 10790826]
25. Sacks MS, Enomoto Y, Graybill JR, et al. In-Vivo Dynamic Deformation of the Mitral Valve Anterior Leaflet. Annals of Thoracic Surgery. 2006; 82:1369–1377. [PubMed: 16996935]
26. Bogen DK, Rabinowitz SA, Needleman A, McMahon TA, Abelmann WH. An analysis of the mechanical disadvantage of myocardial infarction in the canine left ventricle. Circulation Research. 1980; 47:728–741. [PubMed: 7418131]
27. Gupta KB, Ratcliffe MB, Fallert MA, Edmunds LH, Bogen DK. Changes in passive mechanical stiffness of myocardial tissue with aneurysm formation. Circulation. 1994; 89:2315–2326. [PubMed: 8181158]
28. Pilla JJ, Gorman JH III, Gorman RC. Theoretical Impact of Infarct Compliance on Left Ventricular Function. Annals of Thoracic Surgery. 2009; 87:803–811. [PubMed: 19231393]
29. Ratcliffe MB. Non-Ischemic Infarct Extension: A New Type of Infarct Enlargement and a Potential Therapeutic Target. Journal of the American College of Cardiology. 2002; 40:1168–1171.
30. Narula N, Narula J, Zhang PJ, et al. Is the Myofibrillarlytic Myocyte a Forme Fruste Apoptotic Myocyte? Annals of Thoracic Surgery. 2005; 79:1333–1337. discussion 1337. [PubMed: 15797072]
31. Wilson EM, Moainie SL, Baskin JM, et al. Region and Type Specific Induction of Matrix Metalloproteinases in Post Myocardial Infarction Remodeling. Circulation. Jun 10.2003 107:2857–2863. [PubMed: 12771000]
32. Christman KL, Lee RJ. Biomaterials for the treatment of myocardial infarction. Journal of the American College of Cardiology. 2006; 48:907–913. [PubMed: 16949479]
33. Christman KL, Vardanian AJ, Fang QZ, Sievers RE, Fok HH, Lee RJ. Injectable fibrin scaffold improves cell transplant survival, reduces infarct expansion, and induces neovasculature formation in ischemic myocardium. Journal of the American College of Cardiology. 2004; 44:654–660. [PubMed: 15358036]
34. Singelyn JM, DeQuach JA, Seif-Naraghi SB, et al. Naturally derived myocardial matrix as an injectable scaffold for cardiac tissue engineering. Biomaterials. 2009; 30:5409–5416. [PubMed: 19608268]
35. Fujimoto KL, Ma ZW, Nelson DM, et al. Synthesis, characterization and therapeutic efficacy of a biodegradable, thermoresponsive hydrogel designed for application in chronic infarcted myocardium. Biomaterials. 2009; 30:4357–4368. [PubMed: 19487021]
36. Li W, Tanaka K, Ihaya A, et al. Gene Therapy for Chronic Myocardial Ischemia Using Platelet-Derived Endothelial Growth Factor in Dogs. American Journal of Physiology. 2005; 288:H408–H415. [PubMed: 15374822]
37. Laflamme MA, Zbinden S, Epstein SE, Murry CE. Cell-Based Therapy for Myocardial Ischemia and Infarction: Pathophysiological Mechanisms. Annual Review of Pathology: Mechanisms of Disease. 2007; 2:307–339.

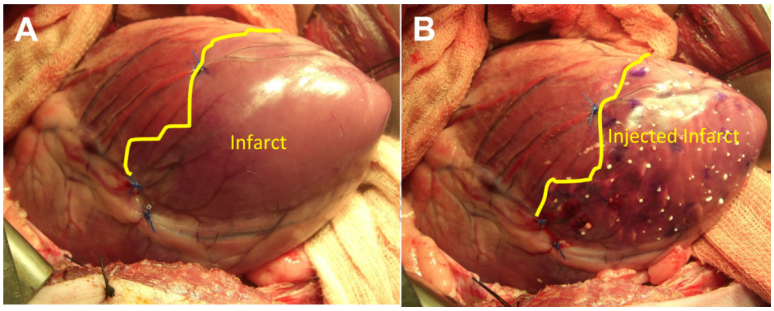

Figure 1.
Sheep heart as seen through a left thoracotomy. Panel **A** is immediately after coronary ligation. Note the discolored apical region in the area of the infarct. Panel **B** is immediately after dermal filler injection.

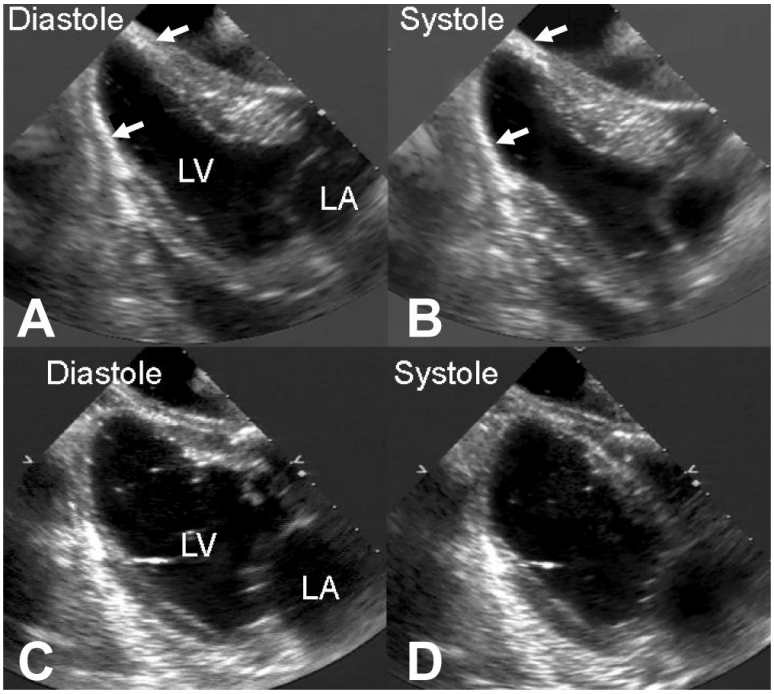

Figure 2.

Representative two-dimensional long-axis echocardiograms in diastole and systole in representative treatment (Panel **A** and **B**) and control (Panel **C** and **D**) hearts 8 weeks after infarction. Note the preservation of the normal elliptical left ventricular shape in the treated heart and the near spherical shape of the control heart. The white arrows identify the radio opaque filler material in the apical region of the treated heart.

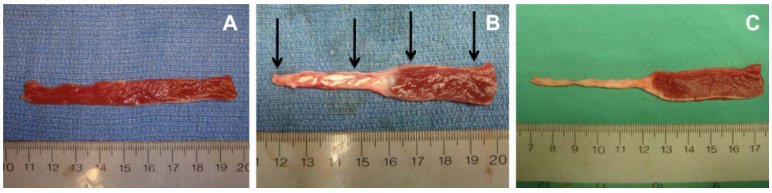

Figure 3.

Representative examples of post-mortem, long axis sections taken from sheep left ventricles to assess regional myocardial thickness. Panel **A** is from a normal uninfarcted heart. Panel **B** is from a treated heart 8 weeks after injection of the tissue filler material and Panel **C** is from and untreated control heart 8 weeks after infarction. The black arrows in Panel **B** indicate were thickness measurements were made. Note the preservation in thickness of the apical region in the treated heart and the profound thinning experienced in the untreated heart.

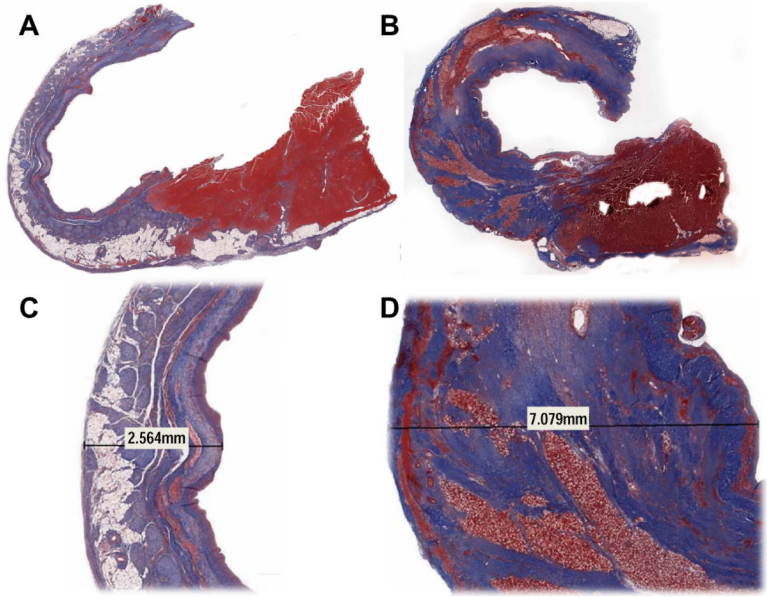

Figure 4.

Masson's trichrome staining in representative control (Panels **A** and **C**) and treatment (Panels **B** and **D**) animals 8 weeks after infarction. Panels **A** and **B** are 1× magnification and Panels **B** and **D** are 1.2×. Notice the exuberant collagen production (blue) and lack of fat infiltration in the treated animal relative to control. The increase in collagen was responsible for most of the increased infarct thickness. Eight weeks after infarction the carrier gel of the tissue filler had been completely absorbed and a cellular (red) infiltrate was left surrounding the calcium hydroxyapatite microspheres.

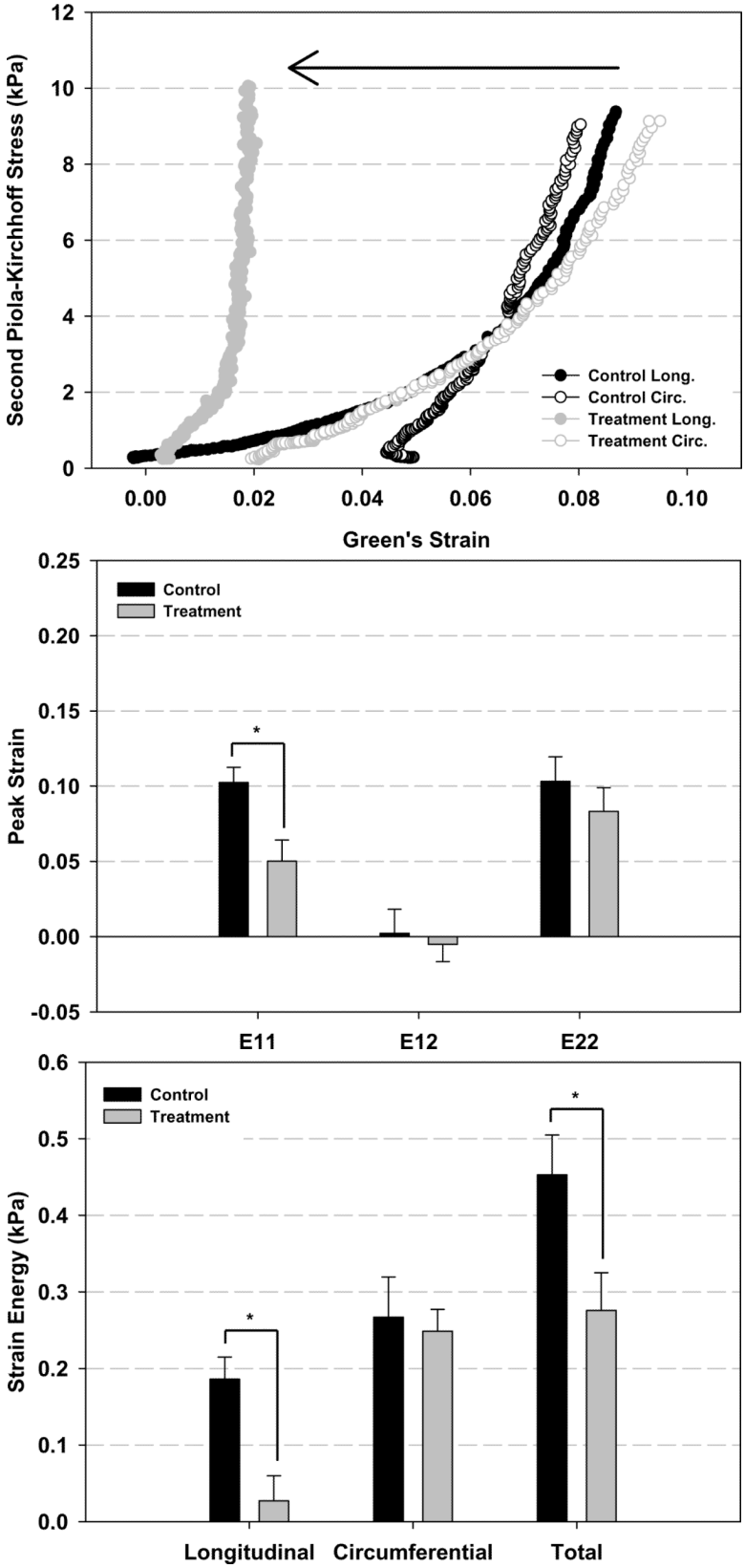

Figure 5.

Results of the mechanical testing of the infarct tissue. Panel **A** presents representative stress-strain plots of specimens from both groups. Panel **B** and Panel **C** depict peak strain and peak strain energy for all groups, respectively. Longitudinal peak strain (E_{11}) was significantly reduced in the treatment group compared to the control group. Total strain energy was also significantly less in the treatment group compared to control. As with the mean peak strain data, the directional strain energies were found to be isotropic in the treatment group and anisotropic in the control group. * $p<0.05$ between group difference: E_{11}- longitudinal strain; E_{22}-Circumferential strain; E_{12}-longitudinal-circunferential shear strain

Table 1

Echocardiographic and Hemodynamic Data

	Pre-MI		Post-MI		Post-Injection		8 Weeks after MI		8 Weeks after MI with Dobutamine	
	Control	**Treatment**	**Control**	**Treatment**	**Control**	**Treatment**	**Control**	**Treatment**	**Control**	**Treatment**
Echocardiographic Data										
ESV (ml)	27.5±1.7	25.2±1.2	43.8±2.6	43.6±2.1	44.6±2.9	41.7±2.4	80.3±6.9	60.8±4.3*	42.1±7.4	32.5±3.1*
EDV (ml)	49.4±1.5	48.9±2.5	66.9±3.4	67.9±2.0	66.0±3.5	64.9±2.7	110.6±8.4	87.2±4.0*	60.6±9.3	50.3±4.3*
EF (%)	44.3±2.9	47.9±2.0	34.6±1.3	36.0±1.9	34.5±1.4	35.5±1.7	27.6±1.3	31.0±2.6*	31.4±1.2	36.0±2.5*
Infarct Length (cm)	--	--	7.2±0.3	7.1±0.3	7.1±0.3	6.8±0.4	9.3±0.6	8.0±0.2*	9.5±0.6	8.2±0.5*
Hemodynamic Data										
Heart Rate	90.9±2.3	92.3±4.3	102.2±3.8	103.0±4.1	104.2±4.7	102.0±4.6	91.7±5.3	92.9±3.3	199.3±7.6	220.2±3.2*
Systolic LV Pressure (mmHg)	101.3±5.3	103.3±1.5	100.3±4.4	99.3±3.6	98.3±2.7	99.3±8.0	96.3±7.6	98.3±4.7	87.3±7.7	91.3±3.7
Diastolic LV Pressure (mmHg)	5±2	4±1.5	14.0±4.2	16.1±3.3	14.7±6.2	15.1±5.3	12.3±1.1	9.8±2.4	9.6±3.7	7.7±2.9
Cardiac Output	4.4±0.2	4.7±0.4	2.9±0.6	2.9±0.7	2.8±0.4	3.1±0.2	2.7±0.1	4.2±0.2*	4.8±0.9	6.0±0.3*
CVP	13.4±3.1	12.6±2.4	15±2.9	15±4.9	15±4.9	12±3.9	14.5±1.3	13.4±1.1	12.7±0.8	11.5±1.0

Average values ± standard error of the mean

* $p<0.05$ vs. Control

Table 2

Myocardial Regional Blood Flow Data

	Regional Blood Flow Myocardial at Rest (ml/min/g)			Regional Blood Flow Myocardial with Dobutamine (ml/min/g)		
	Infarct	**Borderzone**	**Remote**	**Infarct**	**Borderzone**	**Remote**
Control	0.11±0.03†	0.78±0.11†	0.75±0.14†	0.14±0.03†	1.68±0.23†	1.45±0.15†
Treatment	0.22±0.04*†	0.51±0.05*	0.48±0.04*	0.43±0.11*†	1.66±0.14†	1.32±0.14†
Uninfarcted	0.51±0.07	0.52±0.07	0.47±0.04	2.25±0.28	2.08±0.22	1.84±0.17

Average values ± standard error of the mean

*p<0.05 vs. Control

†vs. Uninfarcted

Table 3

Post-Mortem Cardiac Morphometric Data

	Weights			Wall Thickness (mm)				
	Body (kg)	**LV (g)**	**RV (g)**	**Infarct (Apical)**	**Infarct (Basilar)**	**Borderzone**	**Remote**	**Infarct Size (% of LV)**
Control	42.2±1.1†	131.8±3.4†	49.2±2.7†	2.2±0.3	4.7±0.4	11.3±0.4	12.4±0.4	28.7±1.0†
Treatment	44.3±0.7	137.5±4.3†	52.4±2.6†	5.5±0.2*	7.1±0.2*	12.2±0.4†	12.9±0.3†	25.8±1.3*†
Uninfarcted	46.2±1.4	115.0±5.4	41.0±2.4	6.1±0.4*	8.5±0.5	10.3±0.6	11.7±0.7	0

Average values ± standard error of the mean;

*p<0.05 vs. Control

†p<0.05 vs. Uninfarcted